

An Improved Model of the Induction Machine Dedicated to Faults Detection - Extension of the Modified Winding Function

A. Ghoggal, M. Sahraoui, A. Aboubou, S.E. Zouzou
 Laboratoire de Modélisation des systèmes Electromagnétique
 Département d'Electrotechnique
 Université Mohamed Khider
 BP.145, Biskra - Algeria
 E-mail: ghoetudes@yahoo.fr

H. Razik
 Groupe de Recherches en Electrotechnique
 et Electronique de Nancy GREEN - UHP - UMR - 7037
 Université Henri Poincaré - Nancy 1 - BP 239
 F - 54506 Vandœuvre-lès-Nancy, Cedex, France
 E-mail: Hubert.Razik@ieee.org

Abstract—This paper deals mainly with the modelling of induction machine inductances by taking into account all the space harmonics, the introduction of the skewing rotor bars effects and linear rise of MMF across the slot. The model is established initially in the case of symmetric machine, which corresponds to the case of a constant air-gap. Then in other cases where the machine presents a static or dynamic eccentricity, an axial or radial eccentricity. This objective would be achieved by exploiting an extension in 2-D of the modified winding function approach (MWFA). Moreover, the theoretical aspects are presented and the stator current spectra analysis proves the effectiveness of this approach in case of eccentricity.

I. INTRODUCTION

The multiple coupled circuit, defined in the aim of approaching the real structure of the rotor cage, supposes that this one gathers round a number of loops forming a polyphase winding. Each loop consists of two adjacent bars and the two portions of the end ring which connect them [1]. Such a structure was used in aid of the induction machine diagnosis. Several studies were carried out in this axis, and made possible to reveal some phenomena rising from a defect. Such higher or lower sideband frequencies appear in the stator frequency spectral analysis of the line currents, the torque, the speed and the power. Some papers suppose a perfect distribution of the MMF in the air-gap, others adopt models taking into account the real distribution of machine's windings [2]. In particular with the implication of winding function, then, MWFA [3], it is possible to detect some phenomena accompanying a probable eccentricity. Finally, the introduction of the axial dimension was used [4], [5]. This approach takes advantage to define inductances of a machine by taking into account the skew of the slots, and it can be extended to the study of other types of axial asymmetries, namely, the axial eccentricities.

In this work, a 2-D model of the induction machine will be approached while focusing the study on its first aim; the modelling of induction machine inductances with non-sinusoidal distribution of the stator winding, the axial and radial non-uniformity of the air gap. The study will be based on an extension of the MWFA, simulation results as well as comments will be exposed.

II. A 2-D PRESENTATION OF THE MODIFIED WINDING FUNCTION APPROACH

To formulate the problem, we refer to the Fig. 1 which gathers together two cylindrical masses separated by an air-gap. One of it is hollow out and represents the stator, and the other represents the rotor. An $abcd$ arbitrary contour is defined thanks to a reference frame fixed on the stator, to an axial reference and to the mechanical position of the rotor measured by respecting a fixed stator reference. At a rotor position θ_r are defined the angles $\varphi_0 = 0$, $z_0 = 0$ and they are located by the points a and b , and by the same way, the angle φ and the length z are located by using the points c and d . On another side, a and d are located on the stator inner surface, and b and c on the rotor external surface.

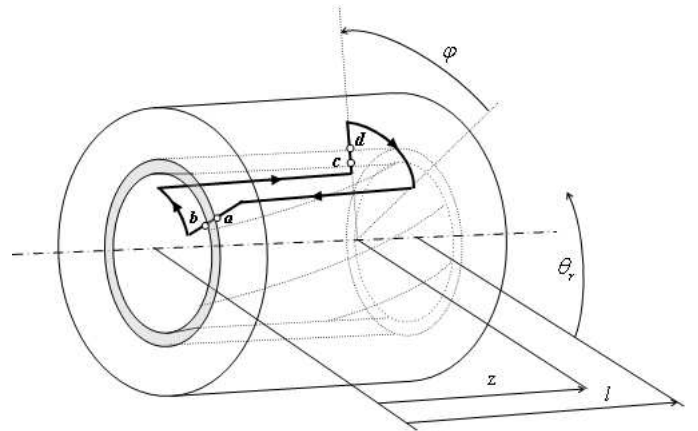


Fig. 1. Elementary induction machine

Let us extend the approaches proposed in [3] by using the axial dimension. Thus, according to the Gauss's law, the integral of the magnetic flux density on closed surface S of a cylindrical volume defined in comparison to the average radius of the air-gap r is null

$$\oint_S \mathbf{B} \cdot d\mathbf{s} = 0 \quad (1)$$

By defining, at any of coordinates (φ, z) , the magnetic field intensity \mathbf{H} , the magnetomotive force F and the effective air-

gap function g , such as $B = \mu_0 H$ and $H = F/g$, the Eq. (1) becomes

$$\mu_0 r \int_0^{2\pi} \int_0^l \frac{F(\varphi, z, \theta_r)}{g(\varphi, z, \theta_r)} dz d\varphi = 0 \quad (2)$$

where l is the effective length of the air-gap. On another side, and according to the Amper's law, it is possible to write

$$\oint_{abcd} H(\varphi, z, \theta_r) dl = \int_{\Omega} J ds \quad (3)$$

Ω is a surface enclosed by the closed path $abcd$, and J the current density. According to the MMF and the number of turns enclosed by the closed path $abcd$ and traversed by the same current i , (3) can be written as

$$F_{ab}(0, 0, \theta_r) + F_{bc} + F_{cd}(\varphi, z, \theta_r) + F_{da} = n(\varphi, z, \theta_r) i \quad (4)$$

where $n(\varphi, z, \theta_r)$ is called the 2-D spatial winding distribution [5], or the 2-D turns function.

By considering the permeability of the iron as infinity, F_{bc} and F_{da} are null. The substitution of these values in (4) gives

$$F_{cd}(\varphi, z, \theta_r) = n(\varphi, z, \theta_r) i - F_{ab}(0, 0, \theta_r) \quad (5)$$

By introducing the average value of the inverse air-gap function $\langle g^{-1}(\varphi, z, \theta_r) \rangle$ with

$$\langle g^{-1}(\varphi, z, \theta_r) \rangle = \frac{1}{2\pi} \int_0^{2\pi} \left[\frac{1}{l} \int_0^l g^{-1}(\varphi, z, \theta_r) dz \right] d\varphi \quad (6)$$

and while exploiting (2) and (5), it will be possible to lead to the expression giving $F_{cd}(\varphi, z, \theta_r)$ such as

$$F_{cd}(\varphi, z, \theta_r) = n(\varphi, z, \theta_r) i - \frac{1}{2\pi l \langle g^{-1}(\varphi, z, \theta_r) \rangle} \int_0^{2\pi} \int_0^l n(\varphi, z, \theta_r) g^{-1}(\varphi, z, \theta_r) i dz d\varphi \quad (7)$$

The 2-D winding function can be obtained by dividing the members of (7) by the current i

$$N(\varphi, z, \theta_r) = n(\varphi, z, \theta_r) - \frac{1}{2\pi l \langle g^{-1}(\varphi, z, \theta_r) \rangle} \int_0^{2\pi} \int_0^l n(\varphi, z, \theta_r) g^{-1}(\varphi, z, \theta_r) dz d\varphi \quad (8)$$

It is to be noticed that this new expression does not hold any restriction as for the axial uniformity, in particular in term of skewed slots and axial air-gap non uniformity.

III. CALCULATION OF INDUCTANCES

A. Machine with uniform air-gap

Firstly, we suppose that the machine is symmetrical. The air-gap length g is reduced to g_0 which is the average value of the radial air-gap length in the case of no eccentricity. Defining F the MMF distribution in the air-gap due to the current i_{A_i} flowing in an arbitrary coil A_i , the elementary flux corresponding in the air-gap is measured in comparison to an elementary volume of section ds and length g_0 such as

$$d\phi = \mu_0 F g_0^{-1} ds \quad (9)$$

The calculation of total flux is made through a calculation of a double integral. By carrying out the change of variable $x = r\varphi$ and $x_r = r\theta_r$, the study is transformed to a reference with axes X and Z where we can imagine a plane representation of the machine. It is clear that, in this case, x translates correctly the linear displacement along the arc corresponding to the angular opening φ . It is the same thing concerning x_r and θ_r .

Knowing that N is the MMF per unit of current, the expression giving the flux seen by all the turns of coil B_j of winding B due to i_{A_i} flowing in coil A_i will be reduced as

$$\phi_{B_j A_i} = \frac{\mu_0}{g_0} \int_{x_{1j}}^{x_{2j}} \int_{z_{1j}(x)}^{z_{2j}(x)} N_{A_i}(x, z, x_r) n_{B_j}(x, z, x_r) i_{A_i} dz dx \quad (10)$$

That is due to the fact that by taking account the axial asymmetry, $n_{B_j}(x, z, x_r)$ will be defined so as to be able to translate the skew of the slots. In 2-D, it will be written in the following way

$$n_{B_j}(x, z, x_r) = \begin{cases} w_{B_j} & x_{1j} < x < x_{2j}, z_{1j}(x) < z(x) < z_{2j}(x) \\ 0 & \text{in the remaining interval} \end{cases} \quad (11)$$

where w_{B_j} is the number of turns of coil B_j . It is equal to 1 in the case of a rotor loop. Generally, the total flux ψ_{BA} relating to all coils composing winding A and B holds its general expression by integrating over the whole surface. And knowing that the mutual inductance L_{BA} is the flux ψ_{BA} per unit of the current, it yields

$$L_{BA}(x_r) = \frac{\mu_0}{g_0} \int_0^{2\pi} \int_0^l N_A(x, z, x_r) n_B(x, z, x_r) dz dx \quad (12)$$

Let us notice that a rearrangement of (12) makes possible to define an inductance in per unit of the length as described in [4]

$$L_{BA}(x_r) = \int_0^l L'_{BA}(z, x_r) dz \quad (13)$$

In the same way as [1], and according to the manner of connections of the coils translated by the sign in (14), this inductance can be obtained by summing all mutual inductances between the q and p coils of winding A and B respectively, such as

$$L_{BA}(x_r) = \sum_{i=1}^q \sum_{j=1}^p \pm L_{B_j A_i}(x_r) \quad (14)$$

B. Bars skewing

Figure 2 depicts the crossing of a rotor loop r_j under the field of a stator coil A_i . The skew is written thanks to the definition of $z(x)$ (10) which will be a function describing the uniform skew, or particularly, the case of spiral skew.

We can notice that the pitch α_{A_i} of the coil A_i is defined in comparison to its sides placed at $x_{1i} = r\varphi_{1i}$ and $x_{2i} = r\varphi_{2i}$, and that the effect of linear rise of MMF across the slot is note represented in this figure.

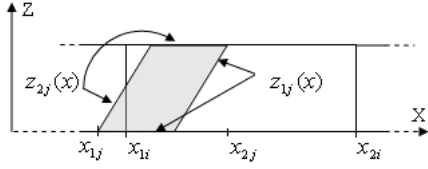


Fig. 2. Representation of the skew

C. Slot opening

Let us examine the case of coil A_i with w_{A_i} turns placed in slots which can present an opening of the width β according to the configuration considered. Figure 3 shows the turns function of coil A_i when the slot opening is taken into account in the calculation using a linear rise of the MMF across the slot.

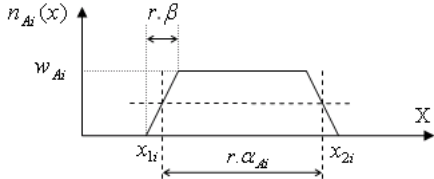


Fig. 3. Turns function of coil A_i

D. Machine with an eccentric rotor

Equation (12) takes its generalized form as

$$L_{BA}(x_r) = \mu_0 \int_0^{2\pi r l} \int_0^l N_A(x, z, x_r) n_B(x, z, x_r) g^{-1}(x, z, x_r) dz dx \quad (15)$$

With the use of (14) and (15), it will be possible to calculate all inductances of the machine where the inverse of the air-gap expression is defined by

$$g^{-1} = g^{-1}(x, x_r) \quad : \text{in case of a purely radial eccentricity}$$

$$g^{-1} = g^{-1}(x, z, x_r) \quad : \text{in case of eccentricity along axis } z$$

where g is giving by its general expression as follows

$$g(x, z, x_r) = \frac{r}{g_0} [1 - \delta_s(z) \cos(x/r) - \delta_d(z) \cos((x - x_r)/r)] \quad (16)$$

where δ_s and δ_d are the amount of static and dynamic eccentricity respectively which are function of z . A numerical calculation makes possible to find the integral (15), however, an analytical resolution must call upon an approximated expression of g^{-1} by carrying out a development in Fourier series. A perfect result would be obtained while stopping at the third term, such as

$$g^{-1}(x, z, x_r) \approx P_0(z) + P_1(z) \cos(x/r - \rho) + P_2(z) \cos(2(x/r - \rho)) \quad (17)$$

ρ and coefficients P_0 , P_1 and P_2 are calculated from g_0 , $\delta_s(z)$, $\delta_d(z)$ and θ_r like describing in [6] and [7]. It is to be recalled that for any winding A and B , equality $L_{AB} = L_{BA}$ is always checked [6]. All inductances are calculated at each time. They used an average radius of the air-gap r in the case or not of eccentricity, which can admit of variations of the air-gap

radius R due to the eccentricity. These one are negligible in front of the average radius itself. Nevertheless, it is not the true concerning the air-gap. Consequently, the ratio can be rewritten as

$$\frac{R(x, z, x_r)}{g(x, z, x_r)} = \frac{r \pm \Delta R(x, z, x_r)}{g_0 \pm \Delta g(x, z, x_r)} \approx \frac{r}{g_0 \pm \Delta g(x, z, x_r)} \quad (18)$$

IV. SIMULATION RESULTS

A. Machine with uniform air-gap

The first induction machine studied in this paper is a three-phase, 4-pole motor [4], whose parameters appear in the Appendix. The structure of the stator coils is presented in the Fig. 4, where only the phase A is considered. Each circle represents the section of an elementary coil of w turns. A , B , and C are the three stator phases, and r_j is the j^{th} rotor loop.



Fig. 4. Winding of the stator phase A

Figure 5 illustrates the functions which describe the mutual inductances L_{r1A} between the first stator phase A and the first rotor loop. The four cases are considered with or not the taking into account the slots opening and the rotor bars skewing. A rotor loop is seen as being one coil with one turn. We have to notice that the mutual inductance between phase A and the seconde rotor loop is identical to the first loop but shifted to the left by the angle $2\pi/Nb$. Thus, the other inductances, L_{r1B} and L_{r1C} are identically reproduced, but shifted to the right by the angle $\pi/3$. The mechanical skewing angle of the rotor bars is $\gamma = \pi/12rad$, which is selected equal to one stator slot pitch. The width of the slot opening is $\beta = \pi/24rad$. In each figure, the function whose maximum value is the most significant, represents the first derivative of the mutual inductance L_{r1A} .

The self inductances and the mutual inductances between windings of the same frame (stator or rotor) are not affected by the skew effect. However, a variation of the stator inductances values is appeared. This is due to the taking into account of the linear rise of MMF across the slot (Table I).

B. Machine with an eccentric rotor

1) *Radial eccentricity*: The second specific induction motor studied is a three-phase, 11kw, 50Hz, 4-pole motor, having four coils per phase group, eight coils per phase, series connected [8]. The others parameters are given in the Appendix. Figures 6-11 show the results of simulation for different degrees of eccentricity, and with three terms P_0 , P_1 and P_2 used in the development of g^{-1} .

TABLE I
STATOR INDUCTANCES

	L_A (H)	L_{AB} (H)
$\beta = 0$	0.1198	-0.0532
$\beta = \pi/24$	0.1165	-0.0529

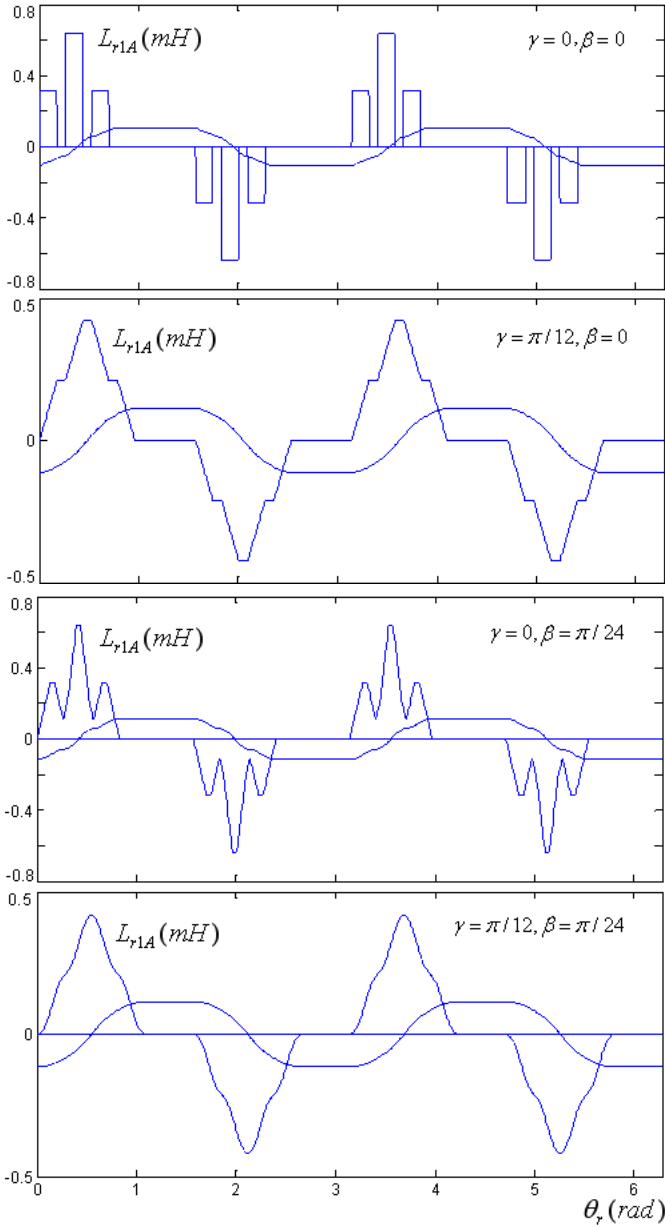


Fig. 5. Mutual inductance between stator phase A and rotor loop r_1

C. Axial eccentricity

To examine the case of the static eccentricity, the expression of $\delta_s(z)$ must be defined. According to Fig. 12 showing the external diameter of the rotor and the internal diameter of the stator with exaggeration in the representation of the air-gap, $\delta_s(z)$ can be written as

$$\delta_s(z) = \delta_{s0} \left(1 - \frac{z}{L}\right). \quad (19)$$

As presented in Fig. 12, the minimum air-gap for $z = 0$ is supposed at $\varphi = 0$ along the vertical axis. The minimal air-gap has a fixed angular position for the different values of z lesser than L , but its value depends on z .

On another side, if the perfectly concentric section of the

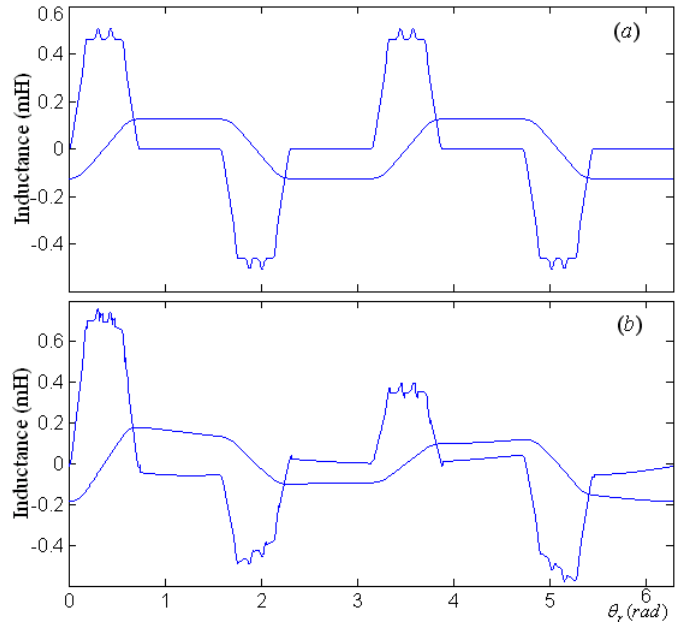


Fig. 6. L_{r1A} and $\frac{dL_{r1A}}{d\theta_r}$: (a) symmetric machine, (b) $\delta_s = 35\%$, $\delta_d = 0\%$

rotor corresponds to $z = L$, thus, the modelling of the eccentricity, L must be selected greater than a certain value guaranteeing the existence of an air-gap with $g(x, z, x_r) \neq 0$ along the rotor length. For $L \rightarrow +\infty$, as a result $\delta_s(z) \rightarrow \delta_{s0}$, and the study is identical to the case of a radial eccentricity. Figure 13 shows the mutual inductance between stator phase A and the first rotor loop with rotor position with $\delta_{s0} = 70\%$ and $L = l/2$.

D. Operation under condition of mixed eccentricity

Knowing that the squirrel cage can be viewed as identical and equally spaced rotor loops, it is possible to establish voltage equations of stator and rotor loops as [1], [2]:

$$[U_s] = [R_s] [I_s] + \frac{d[\psi_s]}{dt} \quad (20)$$

$$[\mathbf{0}] = [R_r] [I_r] + \frac{d[\psi_r]}{dt} \quad (21)$$

$$[\psi_s] = [L_{ss}] [I_s] + [L_{sr}] [I_r] \quad (22)$$

$$[\psi_r] = [L_{rs}] [I_s] + [L_{rr}] [I_r] \quad (23)$$

The vector $[U_s]$ corresponds to the stator voltages, $[I_s]$ and $[I_r]$ to the stator and rotor currents. m is the number of stator phases and N_b the number of rotor bars. $[R_s]$ is an m dimensional diagonal matrix, $[L_{ss}]$ is an $m \times m$ symmetric matrix, $[L_{sr}]$ is an $m \times (N_b + 1)$ matrix, and $[R_r]$ and $[L_{rr}]$ are $(N_b + 1) \times (N_b + 1)$ matrix. Adding to these equations the mechanical expression and the equation of the electromagnetic torque yields to

$$C_e - C_r = J_r \frac{d\omega_r}{dt}, \quad C_e = \left(\frac{dW_{co}}{d\theta_r} \right) \Big|_{(I_s, I_r = \text{constant})} \quad (24)$$

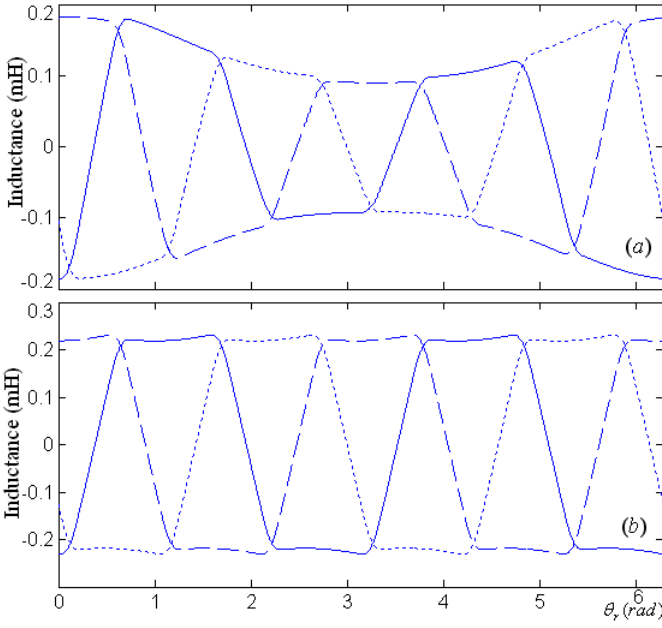


Fig. 7. Mutual inductances L_{r1A} , L_{r1B} , L_{r1C} : (a) $\delta_s = 35\%$, $\delta_d = 0\%$, (b) $\delta_s = 0\%$, $\delta_d = 50\%$

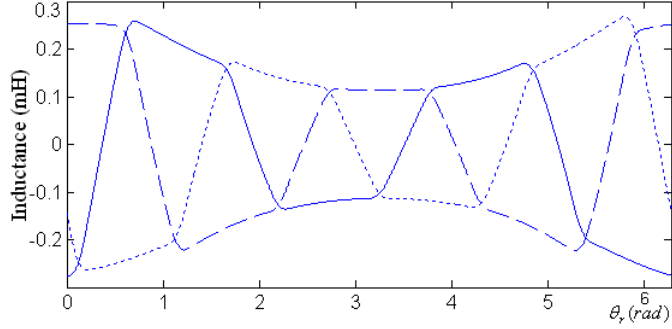


Fig. 8. L_{r1A} , L_{r1B} , L_{r1C} in case of mixed eccentricity of $\delta_s = 35\%$ and $\delta_d = 25\%$

and

$$W_{co} = \frac{1}{2}([I_s]^T[L_{ss}][I_s] + [I_s]^T[L_{sr}][I_r] + [I_r]^T[L_{rr}][I_r] + [I_r]^T[L_{rs}][I_s]) \quad (25)$$

where W_{co} is the coenergy, C_e the electromagnetic torque, C_r the load torque, J_r the rotor load inertia, and ω_r is the mechanical speed of the rotor. Figure 14 shows the simulation result of the operation of machine (2) under conditions of mixed eccentricity of $\delta_s = 40\%$, $\delta_d = 20\%$.

In the spectra of Fig. 14 relating to the current of the first stator phase, it is possible to see the first components which are function of the static eccentricity. This result is derived from the general equation given in [7], and described by

$$f_{slot+ecc} = f_s \left(\frac{N_b}{p} (1-s) \pm 1 \right) \quad (26)$$

f_s represents the main frequency and s the slip in per unit. In the low frequency, components near the fundamental show

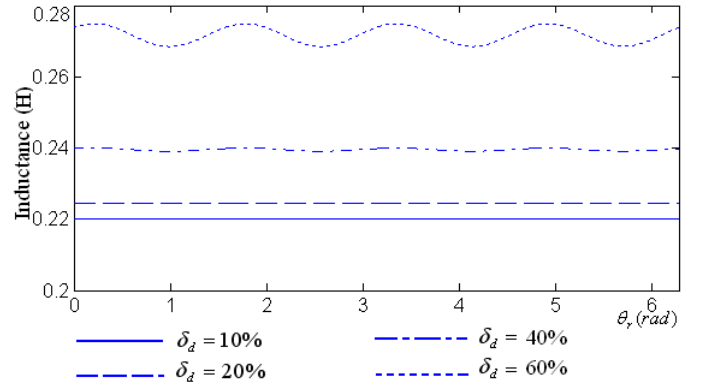


Fig. 9. Self inductance of phase A for different degrees of dynamic eccentricity

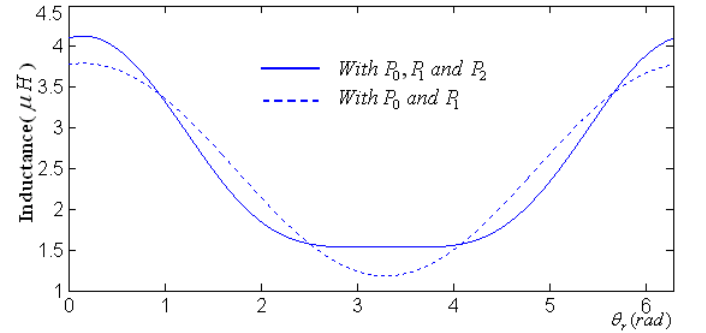


Fig. 10. Self inductance of rotor loop r_1 for 50% of static eccentricity

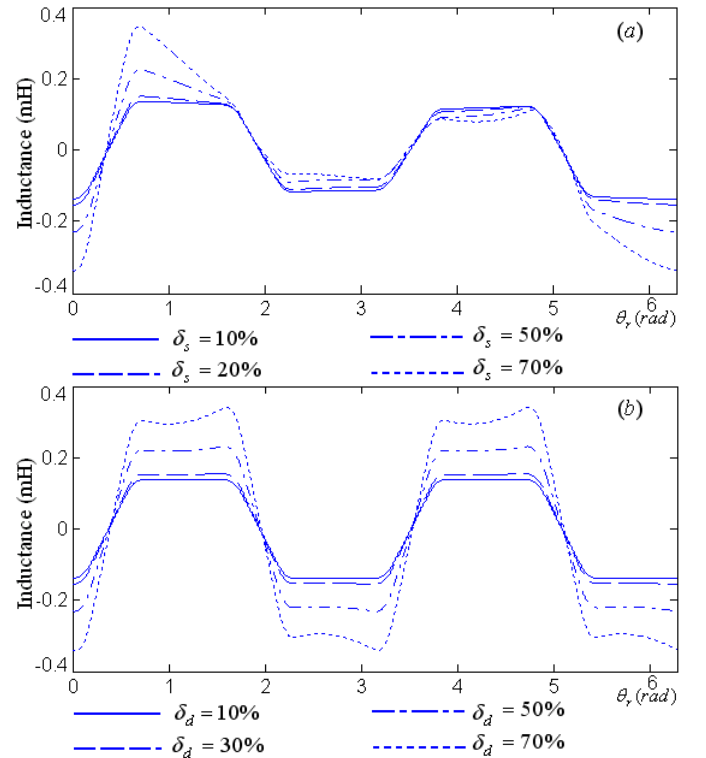


Fig. 11. Mutual inductance L_{r1A} for different degrees of eccentricity: (a) Static eccentricity, (b) Dynamic eccentricity.

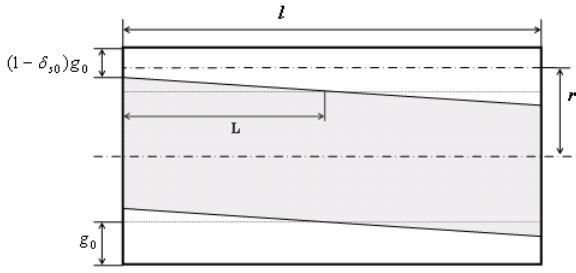


Fig. 12. Illustration of the axial eccentricity

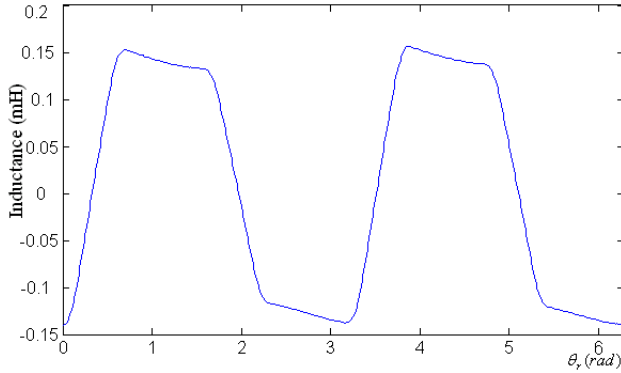


Fig. 13. L_{r1A} for $\delta_{s0}=70\%$ and $L=l/2$

up. This result is as predicted in [8] and described by

$$f_{ecc} = f_s \left(1 \pm \frac{1-s}{p} \right) \quad (27)$$

V. CONCLUSION

In this work, the bases of MWFA were presented with introduction of the axial dimension. It was applied in the calculation of the induction machine inductances with, initially, taking into account of all the space harmonics due to the nonsinusoidal distribution of the MMF in the air-gap. Secondly, we took into consideration the effects generated by the skew and the linear rise of MMF across the slots. Then finally, the modelling of these inductances in the case of air-gap eccentricity conditions are presented (cases of: static, dynamic, radial and axial eccentricity). For that, a simulation tools was established. The spectral components in the stator current allow to identify eccentricity faults. The obtained results were compared with the final results of [4] and [9], and a good agreement was noted. Now, it is advisable to integrate the magnetic saturation effect, and to envisage other faults conditions. It is our work perspective.

APPENDIX

Machines Parameters

-Machine (1) : $g_0 = 0.0006m$, $r = 0.066m$, $l = 0.115m$, $w = 20$, $N_b = 36$, $N_e = 24$.

- Machine (2) : $g_0 = 0.0008m$, $r = 0.082m$, $l = 0.11m$, $w = 28$, $N_b = 40$, $N_e = 48$, $L_b = 95nH$, $L_e = 18nH$, $R_s = 1.75\Omega$, $R_b = 31\mu\Omega$, $R_e = 2.2\mu\Omega$, $J_r = 0.0754kgm^2$, $\gamma = \pi/20rad$, $\beta = \pi/86rad$

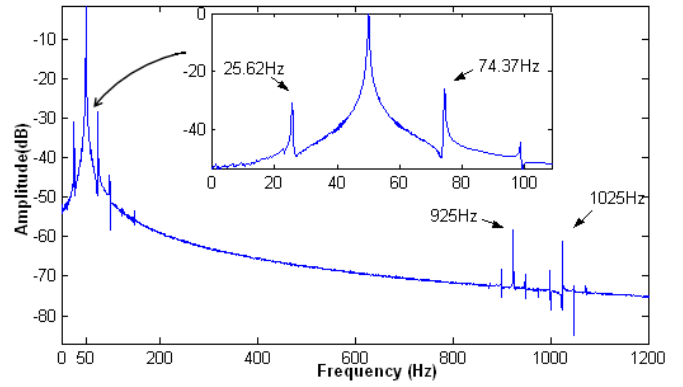


Fig. 14. Stator current spectra with mixed eccentricity condition which are $\delta_s = 40\%$, $\delta_d = 20\%$, $s = 2.5\%$

REFERENCES

- [1] X. Luo, Y. Liao, H.A. Toliyat, A. El-Antably, and T.A. Lipo, "Multiple coupled circuit modeling of induction machines," *IEEE Trans. Industry Applications*, vol. 31, no. 2, pp. 311-318, Mar./Apr. 1995.
- [2] H. A Toliyat, T.A Lipo, "Transient analyse of induction machines under stator, rotor bar and end ring faults," *IEEE Trans. Energy Conversion*, vol. 10, no. 2, pp. 241-247, June 1995.
- [3] N.A. Al-Nuaim and H.A. Toliyat, "A novel method for modeling dynamic air-gap eccentricity in synchronous machines based on modified winding function theory," *IEEE Trans. Energy Conversion*, vol. 13, no. 2, pp. 156-162, June 1998.
- [4] M. G. Joksimovic, D. M. Durovic and A. B. Obradovic, "Skew and linear rise of MMF across slot modeling-Winding function approach," *IEEE Trans. Energy Conversion*, Vol. 14, no. 3, pp. 315-320, Sept. 1999.
- [5] G.Bossio, C.D. Angelo, J.Solsona, G. Garcia and MI. Valla, "A 2-D Model of the induction machine : Extension of the modified winding function approach," *IEEE Trans. Energy Conversion*, vol. 19, no. 1, pp. 144-150, Mar. 2004.
- [6] J. Faiz and I. Tabatabaei, "Extension of winding function theory for nonuniform air gap in electric machinery," *IEEE Trans. Magnetics*, vol. 38, no. 6, pp. 3654-3657, Nov. 2002.
- [7] S. Nandi, R.M. Bharadwaj and H.A. Toliyat, "Performance analyse of three-phase induction motor under mixed eccentricity condition," *IEEE Trans. Energy Conversion*, vol. 17, no. 3, pp. 392-399, Sept. 2002.
- [8] D.G. Dorrell, W.T. Thomson and S.Roach, "Analyse of airgap signals as function of combination static and dynamic airgap eccentricity in 3-phase induction motors," *IEEE Trans. Industry Applications*, vol. 33, no. 1, pp. 24-34, Jan./Feb. 1997.
- [9] M. G. Joksimovic, D. M. Durovic, J. Penman and N. Arthur, "Dynamic simulation of dynamic eccentricity in induction machines-Winding function approach," *IEEE Trans. Energy Conversion*, vol. 15, no. 2, pp. 143-148, June 2000.